




Remote-sensing estimation of the water stress coefficient and comparison with drought evidence

Nesrine Abid ^a, Zoubeida Bargaoui ^a and Chris M. Mannaerts ^b

^aEcole Nationale d'Ingénieurs de Tunis, ENIT Université de Tunis El Manar, Tunis, Tunisia; ^bFaculty of Geo-Information Sciences and Earth Observation (ITC), University of Twente, Enschede, the Netherlands

ABSTRACT

Drought assessment of croplands and sylvo-pastoral areas is crucial in semi-arid regions. Satellite remote sensing offers an opportunity for such assessment. This study presents a method of spatial and temporal estimation of drought index in Medjerda basin (23,700 km²) using satellite data and its validation with in situ investigation of areas with crop damage realized by the ministry of agriculture. To estimate drought index, potential evapotranspiration (PET) is calculated using Penman–Monteith equation and modified FAO-56 crop coefficient (K_c) approach combined with remote-sensing data and actual evapotranspiration is derived from the Meteosat Second Generation platforms. The period of study is the 2010 water year. PET estimations show good accuracy with corrected pan evaporation observations up to 0.9. In comparison, the water stress coefficient (K_s) aggregated by land-cover type shows the coefficient of determination with the fraction of drought damage areas of 0.5 for the third decade of March and first decade of April in croplands areas and 0.8 for the second and third decades of May in croplands and sylvo-pastoral areas. This study showed that satellite data approaches could successfully be used to monitor drought in river basins in the Northern Africa and Mediterranean region.

ARTICLE HISTORY

Received 3 April 2017
Accepted 15 January 2018

KEYWORDS

Drought; stress coefficient (K_s); actual evapotranspiration (AET); NDVI; FVC; satellite application facility (LSA SAF); crop coefficient (K_c)

1. Introduction

Drought is one of the most dangerous natural phenomena in the world. It can have a significant impact on economic and social systems as well as natural ecosystems (Hoerling and Kumar 2003). It causes huge damage to the environment and it is stated as a major cause of land degradation, dryness, and desertification (Masih et al. 2014). The outcome of the drought losses directly affects humanity such as crop failures, food scarcities that may lead to famine, malnutrition, and live losses.

The agro-sylvo-pastoralism sector occupies an important place in the Tunisian economy, as it guarantees the country's food security. The sylvo-pastoralism uses forage trees and shrubs in combination with cultivated species usually cereals (wheat and barley) that is the main agricultural products in northern Tunisia and constitute the 72% of the total surface in the country. According to Boudabous et al. (2000), agro-ecosystems of

Tunisia are located in a climate largely affected by aridity that arises for the whole country with different acuity. Generally, the statistical study indicates that on a 20-year rainfall module, there are, 3 wet years, 6 average years and 11 deficit years (Zahar 1997), which highlights the importance of studying drought risk. The agriculture sector is the first affected by the occurrence of drought, as it is the largest consumer of water resources (about 80% of volume mobilized of water). Therefore, the economy of the study area is very sensitive to the impact of droughts. In order to reduce their resultant effects, national institutions always seek to identify drought. A continuous field survey of the extent of drought is carried out on the croplands and agro-pastoral zones by the ministry of agriculture in order to predict and quantify the drought damage that the governorate must manage. In this context, the accurate assessment of water stress coefficient that reflects the degree of drought can be a valuable tool for drought management.

In recent years, several drought indices are developed and used in order to monitor agricultural drought (Zargar, Sadiq, and Naser 2011). As satellite remote sensing has the advantage of providing regular and synoptic observations of the state of vegetation (normalized difference vegetation index (NDVI), leaf area index, and fraction of vegetation cover (FVC)), and agricultural drought is naturally related to vegetation and soil status (Dalezios, Blanta, and Spyropoulos 2012); several indices based on data derived from optical remote sensors are developed to identify drought (Kogan 1997; Amri et al. 2011). The NDVI is the most commonly used index in vegetation drought monitoring (Brown et al. 2008; Amri et al. 2014). Kogan (1997), Seiler, Kogan, and Wei (2000) and Quiring and Ganesh (2010) tested the Vegetation Condition Index (VCI) in different sites of the world (Africa, America, Europe) and found a high correlation between the VCI and agricultural production and they concluded that VCI could be used to monitor the drought. Also, the Vegetation Anomaly Index (VAI), proposed by Amri et al. (2011), is calculated using data derived from SPOT-Vegetation. The comparison between the NDVI SPOT-Vegetation product and precipitation levels measured at a site situated in the centre of Tunisia (Kairouan plain) shows a good correlation. All these indices are based on the NDVI that shows good accuracies for the quantification of green vegetation cover. The difficulty is that these indices (VCI and VAI) are calculated based on long time series. The Mediterranean Drought Index project (<http://www.onagri.nat.tn/medi/>) proposes to explore the different indicators of drought resulting from observation by remote sensing: VCI, VAI, and the Moisture Anomaly Index, which is calculated on the basis of the Soil Water Index. These indices are available freely for the North part of Africa from 2000 to present the year 2017. According to Ghulam et al. (2007), the NDVI is a reliable indicator of vegetation and moisture conditions (Ji and Peters 2003; Tadesse, Brown, and Hayes 2005). Nevertheless, the occurrence of drought cannot be depicted at once by the NDVI changes because of the delay time. Effectively, drought indices based on NDVI are often a post-effect indicator of drought (Ghulam et al. 2007). Therefore, they cannot be considered as trustworthy indicators when the focus should be on the real-time monitoring of drought conditions.

In our case of study, an alternative method using the water stress coefficient (K_s) proposed by Allen et al. (1998) is selected to assess the drought spatially and temporally. K_s is the ratio of the actual evapotranspiration (AET) to the potential evapotranspiration (PET). K_s decreases with decreasing plant available soil water (Choi et al. 2013). In this context, the estimation of PET and AET is needed. Generally, evapotranspiration is a

dominant term in the water and energy balance. It depends on local climatic conditions (solar radiation, air temperature, and precipitation), the available water content of the soil, water extraction by vegetation, and land use (Allen et al. 1998). The FAO-56 model is the most practical approach used to estimate PET (Allen et al. 1998). It is based essentially on a combination of a reference evapotranspiration value (ET_0) and crop coefficients (K_c). In recent years, this model is combined with vegetation indices derived from optical satellite observations for operational applications (Er-Raki et al. 2007; Er-Raki et al. 2010). On the other hand, several satellite products are developed to assess AET. In this study, the Land Surface Analysis Satellite Applications Facility (LSA SAF) product is selected. It is a surface energy model, which achieves AET using hyper-temporal (30-minute) Meteosat Second Generation (MSG) data and TESSEL (Tiled ECMWF Surface Scheme of Exchange processes at the Land surface) soil vegetation atmosphere transfer, or SVAT model (SAF 2011).

The objective of this research is to evaluate the calculated water stress coefficient using remote-sensing data by confronting it to the result of an investigation realized in the field by the ministry of agriculture for the agriculture year 2009/2010.

2. Study area and data

The study area is the Medjerda basin in northern Tunisia (North Africa). It is bordered to the north and east by the Mediterranean Sea. Its western border opens on Algeria and its southeastern is bordered by Atlas Mountains (Figure 1). It essentially constitutes the

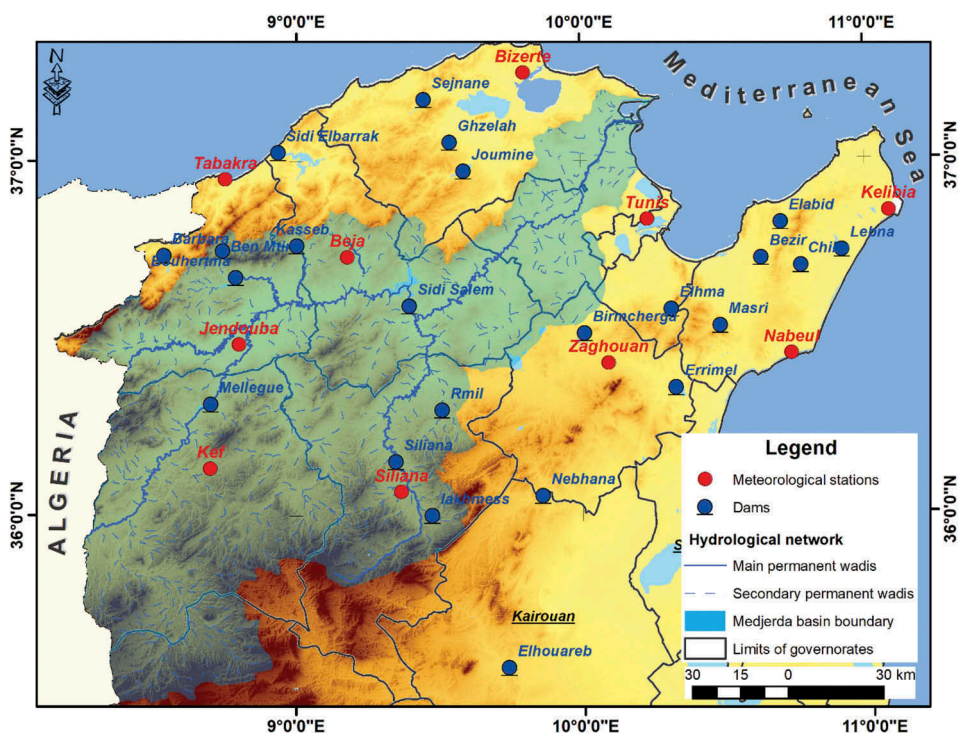


Figure 1. Distribution of meteorological stations and dams with pan evaporation sites.

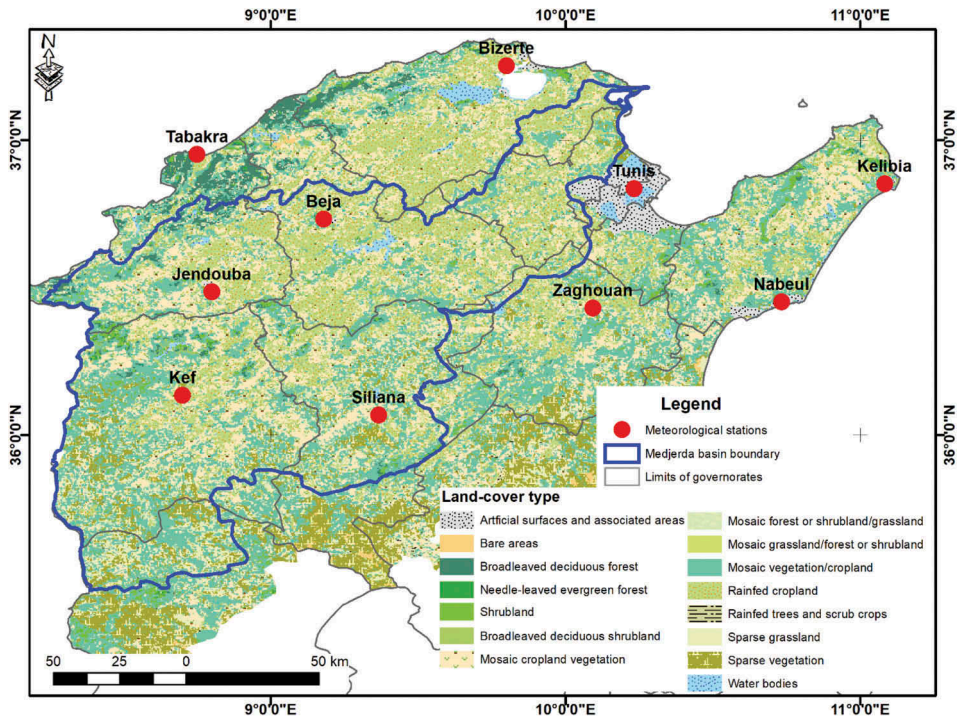


Figure 2. Map of land cover in northern Tunisia (source: www.landcover.org). Sylvo-pastoral areas correspond to the forest lands and the sparse vegetation and grassland.

Tell Tunisia. The climate of the study area divided into humid, subhumid, and semi-arid zones from north to south.

The agroecosystems of the Tell Tunisia is characterized by an abundance of water resources in winter and a deficit in water in summer. Overall, it is characterized by the predominance of an intensive and extensive high-potential agro-sylvo-pastoral production complex. A variety of forests, grasslands, and agricultural practices areas cover the study region (Figure 2).

2.1. *In situ data*

2.1.1. *Assessment of 2010 drought*

The Tunisian authorities have declared that many areas of arable crops in the study area are affected by the drought for the 2009–2010 crop year (from September 2009 to July 2010). These areas are set by state decree No. 2010-1901 of 6 August 2010, which is published in the Official Gazette of the Republic of Tunisia. Such drought assessment is the result of a field investigation realized by the Ministry of agriculture, hydraulic resources, and fisheries in linkage with crop yield. The spatial resolution is by administrative zone called *delegation*, which is the smallest scale used by the authorities to inform about population and socioeconomic data. In the study area, there are 66 *delegations* of size ranging from 40 to 734 km². Figure 3 shows the spatial distribution of delegations as well as the percentage of affected areas in each *delegation* for the

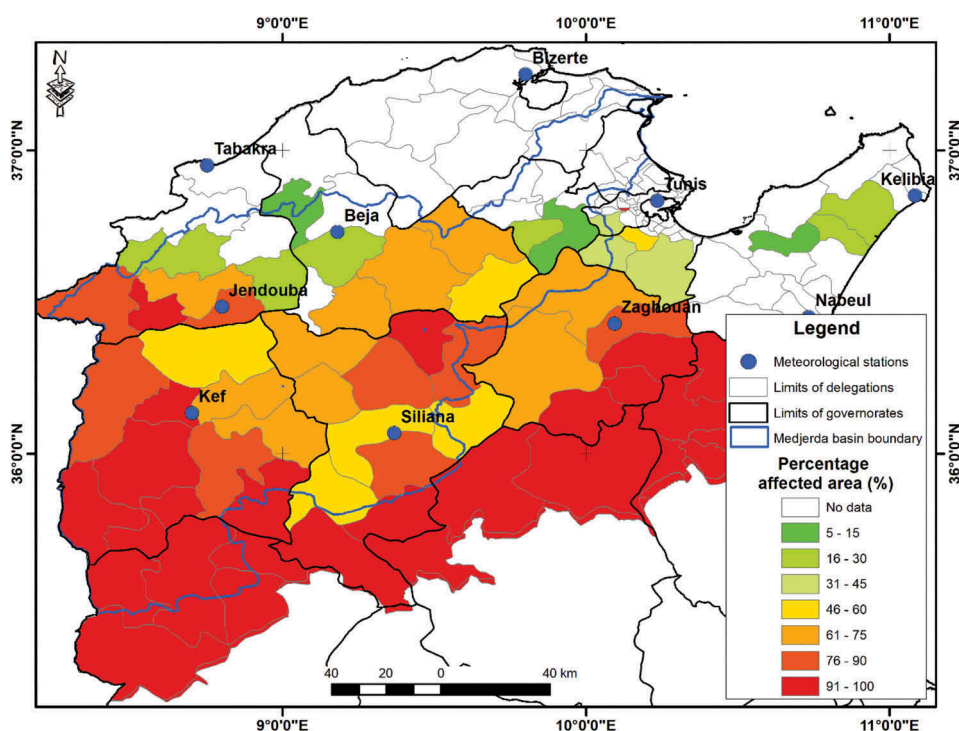


Figure 3. Spatial distribution of the percent of affected areas in each delegation for the Medjerda basin and its surrounding regions declared for the crop year 2009/2010.

Medjerda basin and its surrounding regions. The percentage varies from 5% to 100%, with a north-south gradient. In the northbound, there is no drought while in the south of the basin the drought is everywhere.

2.1.2. Meteorological data

The meteorological data described in Table 1 are provided by the National Institute of Meteorology in Tunisia (www.meteo.tn) for 10 weather stations scattered in northern Tunisia (Figure 1). Four out of 10 are in the Medjerda basin while others are in the surrounding basins. These data are used to estimate daily reference and PET during 2010. Figure 4 highlights the temporal variation of the decadal average of air temperature, relative humidity, and duration of sunshine in four meteorological stations localized in northern Tunisia. The air temperature and the duration of sunshine increase progressively to attend the maximum in the summer, 30°C and 13 h, respectively. The relative

Table 1. Meteorological variables used to calculate reference evapotranspiration (ET_0).

Variable		Unit	Years of observation	Time step
Air temperature	T_a	[°C]	2010	Daily
Air relative humidity	H_r	Percent [%]	2010	Daily
Wind speed	u_2	[$m\ s^{-1}$]	2010	Daily
No. of sunshine hours	N	Hours [hrs]	2010	Daily
Air pressure	P	Pascal [Pa]	2010	Daily

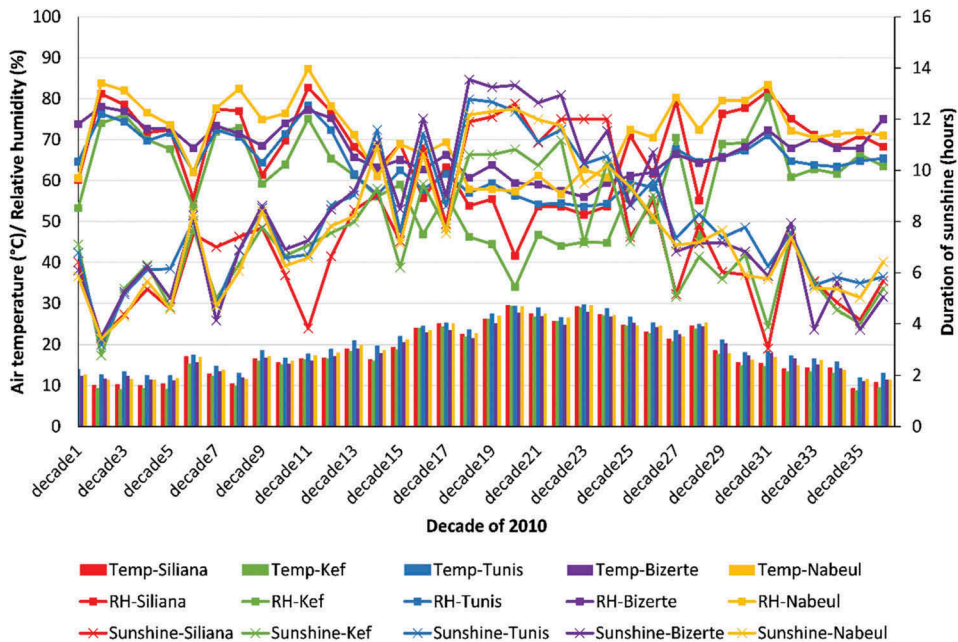


Figure 4. Decadal average air temperature (temp, °C), relative humidity (RH, %), and actual duration of sunshine (hours) in five meteorological stations included in northern Tunisia for the year 2010.

humidity shows an inverse trend with the highest value about 80% in the winter and the lowest value equal to 30% in the summer time.

2.1.3. Pan evaporation data

Daily pan evaporation (PE) data are collected in order to evaluate the accuracy of PET estimations. Data are available from the General Direction of Dams and Large Hydraulic Works, Ministry of Agriculture. The pans locations are showed in Figure 1. The analysis focuses on the first 10 days of March, April, May, and July, a period that includes various stages of crop development and the minimum probability of rain occurrence.

2.2. Remote-sensing data

2.2.1. Vegetation data

Time series of vegetation data NDVI are obtained from SPOT-Vegetation, available from <http://free.vgt.vito.be/>. These data are derived with decadal temporal resolution and 1 km spatial resolution for the year 2010. The FVC comes from LSA SAF product (<https://landsaf.ipma.pt/>) with daily temporal resolution and 3 km spatial resolution. The land cover information is obtained from GlobCover 2009 published by the European Space Agency (http://due.esrin.esa.int/page_globcover.php) with a spatial resolution of 1 km. About 85% of Medjerda basin area is covered by cropland vegetation, rainfed tree, and shrub and 14% of the total area are occupied by sylvo-pastoral activities.

2.2.2. *Meteosat Second Generation evapotranspiration product AET-LSA SAF*

AET LSA SAF product is selected to evaluate AET during 2010 in the study area. The advantage is that it is free. It quantifies the flux of water vapour releases from the ground surface (soil and canopy) into the atmosphere using input data derived from MSG satellites, ECMWF forecasts, and ECOCLIMAP land-cover database (SAF 2011). The physics is based essentially on the TESSEL SVAT model (Viterbo and Beljaars 1995; Van Den Hurk et al. 2000).

The AET LSA SAF product is generated every 30 min with the spatial resolution of 3 km. The daily AET is calculated by temporal integration of 30-min values.

The advantage is that all data could be treated into the ILWIS software environment.

3. Theory and methods

Penman–Monteith (PM) method (Allen et al. 1998) is used to estimate reference and PET.

3.1. *Reference evapotranspiration ET_0*

The FAO-56 PM equation is a physically based combination approach that integrates energy and aerodynamic considerations (Allen et al. 1998). Generally, it gives acceptable ET estimates for practical applications, which require measurement of net radiation, soil heat flux, air temperature, relative humidity, and wind speed. The PM equation also requires knowledge of the canopy resistance. In the following, the calculation of reference evapotranspiration is realized according to the FAO-56 (Allen et al. 1998).

Reference evapotranspiration (ET_0) is the potential ET from a hypothetical green grass of uniform height 0.12 m well watered, and a constant albedo of 0.23 with fixed surface resistance r_s of 70 s m⁻¹ (Allen et al. 1998). The PM equation is as follows:

$$ET_0 = \frac{0.408\Delta(R_n \times G) + \gamma \frac{900}{(T_a + 273)} u_2 (e_s - e_a)}{\Delta + \gamma(1 + 0.34u_2)} \quad (1)$$

where,

ET_0 = reference evapotranspiration (mm day⁻¹),

R_n = the net radiation at the crop surface (MJ m⁻² day⁻¹),

G = soil heat flux density (MJ m⁻² day⁻¹), assumed zero on daily basis,

T_a = mean daily air temperature at 2 m height (°C),

u_2 = wind speed at 2 m height (m s⁻¹),

e_s = saturation vapour pressure (kPa),

e_a = actual vapour pressure (kPa),

$e_s - e_a$ saturation vapour pressure deficit (kPa),

Δ = slope vapour pressure curve (kPa °C⁻¹),

γ = psychrometric constant (kPa C⁻¹)

The reference evapotranspiration (ET_0) is calculated at the level of the meteorological station and then an interpolation using the moving average method under ILWIS environment is adopted.

3.2. Potential evapotranspiration

PET of a specific land cover or vegetation type is evaluated using the FAO-56 (Allen et al. 1998) crop water requirement approach using a crop coefficient K_c defined as follows:

$$PET_{PM} = (ET_0) \times K_c \quad (2)$$

K_c varies little with climate, but mainly with the characteristics of culture (Pereira, Allen, and Perrier 2006) such as planting dates and seeding, the development and the duration of the growing season. Climatic conditions, especially at the beginning of the growth and the frequency of rainfall or irrigation, are also explaining variables. Crop coefficients provided by the Food and Agriculture Organization (FAO) are established experimentally. The validity of these crop coefficients has been proved by many applications reported in the literature (Allen et al. 2005) and by remote-sensing approaches (Neale, Jayanthi, and Wright 2005).

In the present study, the calculation of the crop coefficient K_c is based on dual crop coefficient approach, which is proposed by (Wright 1982). This approach splits the total crop coefficient into crop transpiration (K_{cb}) and soil evaporation (K_e) fractions (Rocha et al. 2010).

The dual crop coefficient concept expresses K_c as follows:

$$K_c = K_{cb} + K_e \quad (3)$$

The crop transpiration fraction K_{cb} is estimated based on NDVI maps as developed by Rocha et al. (2010) who assume a linear relationship between K_{cb} and NDVI. Additionally, the soil evaporation fraction K_e is calculated using the FVC maps. Therefore, in relation to NDVI and FVC, K_{cb} and K_e are derived as (Rocha et al. 2010) follows:

$$K_{cb} = 1.07 \times \left[1 - \left(\frac{(NDVI)_{max} - (NDVI)}{(NDVI)_{max} - (NDVI)_{min}} \right)^{\frac{0.84}{0.54}} \right] \quad (4)$$

$$K_e = \beta \times (1 - (FVC)) \quad (5)$$

$NDVI_{min}$ and $NDVI_{max}$ are the minimal and maximal values of NDVI according to the satellite map. They are associated respectively with bare soil and dense vegetation. FVC is the fraction of vegetation cover. The coefficient β is estimated empirically and is adjusted based on ancillary or local information (Allen et al. 1998). In this research, the coefficient β is assumed to equal to 0.25. It is based on the occurrence of water supply (≈ 10 days) and the average value of ET_0 (4 mm day^{-1}) during the growing season (Allen et al. 1998).

3.3. Correction of pan evaporation

To evaluate the accuracy of PET of crop and vegetation strata, computed using the PM and FAO-56 K_c model, a comparison with PE in situ data is performed. The problem is how to translate the PE in an assessment of the PET.

According to the literature (Riou and Chartier 1985), the appropriate correction coefficient varies between 0.5 and 0.85. This coefficient varies with soil type, season, and type of pan evaporation used. Following (Hillel 1997), based on direct

measurements and a review of the literature, the coefficient 0.66 is adopted for full cover conditions:

$$PET_{fullcover} = 0.66 \times (PE) \quad (6)$$

$PET_{fullcover}$ is the PET for the full cover conditions.

Since PET is a function of the area covered, the stage of the crop's growth must be taken into account, as indicated by its fractional ground cover. Therefore, Hillel (1997) proposed to adopt the following empirical relationship in fractional ground cover conditions:

$$PET_{potentialcover} = 0.33 \times (1 + (FVC)) \times (PE) \quad (7)$$

FVC is the fraction of vegetation cover and $PET_{potentialcover}$ is the PET for fractional ground cover conditions. It is assigned as PET_{PE} throughout the following sections.

3.4. Assessment of decadal potential and actual evapotranspiration (PET and AET)

The PET is calculated using the satellite vegetation data NDVI and FVC on the daily step. Additionally, the AET derived from LSA SAF product are extracted for the year 2010 and all the 30-min time series are integrated into daily step. Then, for the two products, the decadal sum is realized for the year 2010. All these treatments are established on ILWIS environment.

3.5. Method of assessment and validation of stress coefficient

The motivation of estimating PET and AET is the evaluation of the stress coefficient K_s . The method proposed by Allen et al. (1998) is adopted here. They defined the stress coefficient K_s ($0 \leq K_s \leq 1$) as the ratio of AET and PET:

$$K_s = AET/PET \quad (8)$$

The decadal sums of AET and PET are computed to estimate the stress coefficient K_s with 1 km spatial resolution for the year 2010. Significance of K_s is that when it is much less than 1, we assume drought condition, whereas there is no soil water stress for K_s near to unity.

To evaluate the efficiency of such an estimation, a comparison is established taking into account the map of Figure 3, which displays the spatial distribution of the percentage of affected area (P_a) in each delegation for the Medjerda basin and its surrounding regions declared for the crop year 2009/2010. The fraction of affected area is rescaled using the variable F_a :

$$F_a = \frac{P_{amax} - P_a}{100} \quad (9)$$

where P_{amax} is the maximum P_a value in the map. Thus, F_a values vary between 0 (for drought conditions) and 1 (no drought).

The comparison of K_s to the in situ drought investigation is based on the land-cover type. Firstly, we make a correspondence between K_s and land-cover type by pixel for each study decade. Similarly, correspondence is achieved between F_a and land-cover

type by pixel. Therefore, results are tables, which contain, for every pixel, land-cover type with its corresponding water stress coefficient and F_a . Further, average values of K_s and F_a are estimated for each land-cover type. Then, a comparison of average K_s and average F_a is built based on the coefficient of determination R^2 . If R^2 is greater than 0.7, we assume a good agreement between satellite estimation and field estimation of drought.

As the winter period cannot represent any indication of stress coefficient, the computation of R^2 is performed from the seventh decade to the fiftieth decade of the year. This period corresponds to the springtime, which refers to the mid-crop season and the beginning of the late stage of the crop season.

4. Results and discussion

We first present ET_0 and PET estimations and interpretation of their spatial variability and we discuss their accuracy in comparison to the literature for ET_0 and to field data for PET. Then, we analyse the temporal variability of the ET_0 , PET, and AET estimations by land-use type. Finally, we compare K_s interpretation as drought indicator to drought impact on crops observed on the field.

4.1. Temporal and spatial distribution of reference evapotranspiration ET_0

The reference evapotranspiration (ET_0) is estimated using the FAO-56 PM model. Figure 5 shows a non-uniform distribution of reference evapotranspiration across the study area and across the seasons. In the initial stage (first decade of March), ET_0 follows a north-north-east/south-south-west gradient (Figure 5(a)) with values varying between 2.6 and 6.5 mm day⁻¹ (average equal to 2.5 mm). The lowest values are observed in the extreme east part that corresponds to the Cap Bon region and the greatest values are concentrated in the north part. For the first decade of May, Figure 5(b) highlights an average of 5 mm with values varying between 3 and 7 mm day⁻¹. The greatest values are observed in the coast (northeast) and the extreme south part of the study area. Whereas, the lowest values are concentrated in the northwest and the Cap Bon parts. For the late stage (first decade of September), a north-south gradient is highlighted (Figure 5(c)) with values vary between 3.5 mm day⁻¹ in the northeast region (Cap Bon) and 7 mm day⁻¹ in the extreme northern boundary. Therefore, the ET_0 maps show different configurations and gradients that change in intensity and orientation depending on the decade and the season. This can be explained by the influence of humid air from the Mediterranean region leading to smaller moisture deficit, which could lead to reduced values of evapotranspiration (Baccour et al. 2012).

Baccour et al. (2012) realized an interpolation of reference evapotranspiration calculated using FAO-56 PM method with the ordinary kriging method for Tunisia and leading to 5–10% in estimation error. They consider that such a precision is acceptable especially for a low-density network of meteorological stations (23 stations covering an area of 163,610 km²). Therefore, in our case of study, the result of ET_0 obtained by moving average interpolation method is validated by the result published by Baccour et al. (2012). They identify a dominant north-south gradient that characterizes almost all the maps throughout the year. However, depending on the seasons, the direction of this

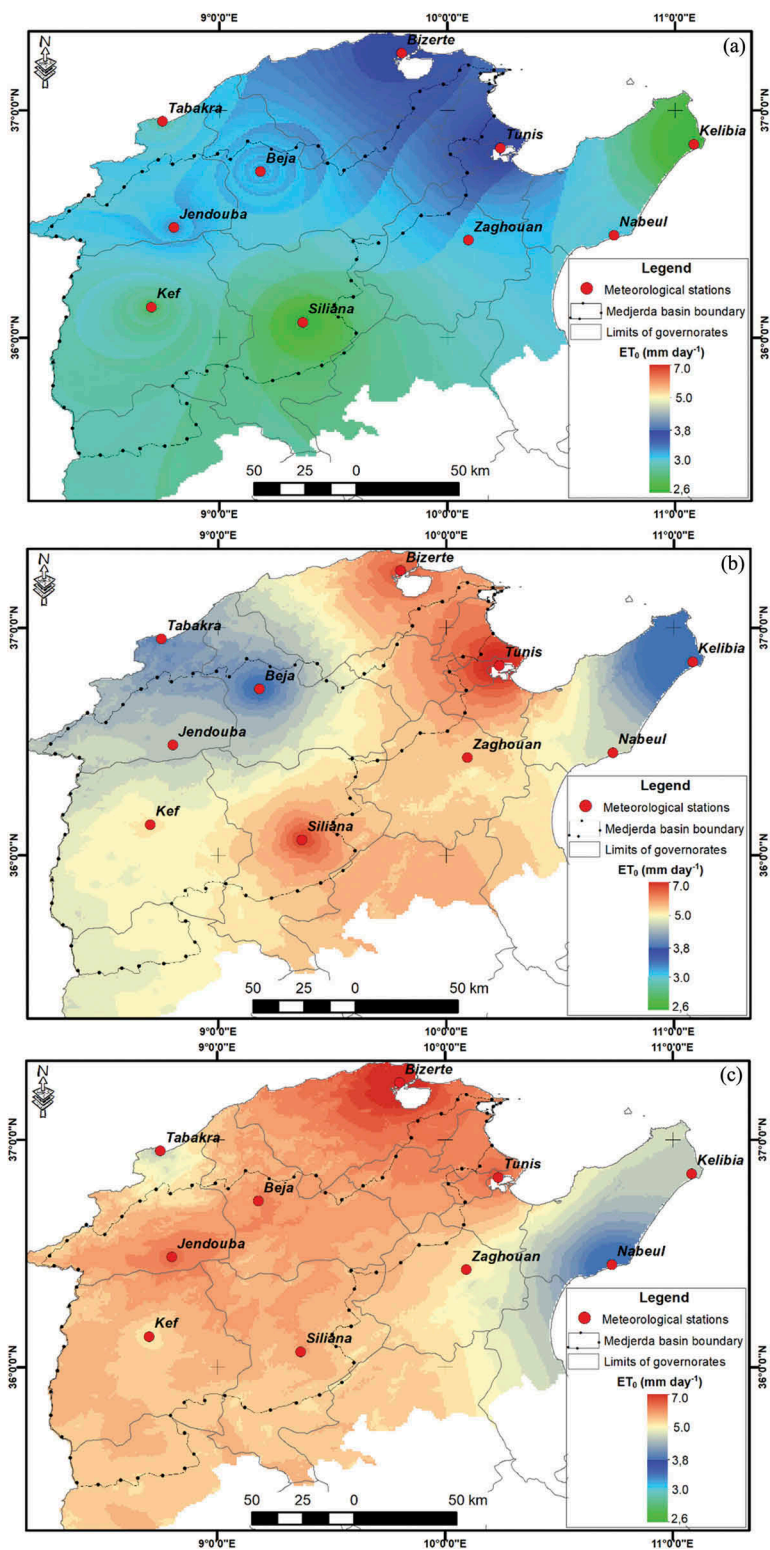


Figure 5. Spatial variability of reference evapotranspiration ET_0 using meteorological in situ data in northern Tunisia for (a) 1 March, (b) 1 May, and (c) 1 September 2010.

gradient is strongly related to the dominant atmospheric currents. Generally, the same behaviour is observed in our ET_0 maps. Additionally, the findings obtained by Habaieb and Masmoudi-Charfi. (2003) for Tunis, Bizerte, and Beja suggested that the highest ET_0 calculated by PM are observed in Bizerte and Tunis regions. The lowest values are recorded in Beja for all months of the year. Our results compare favourably to their results.

4.2. Temporal and spatial distribution of PET

The estimation of the crop coefficients (K_c) based on NDVI and FVC maps resulted in gradients from south to north and northeast to the southwest (Figure 6). The highest values are located in the north part of the Medjerda basin with $K_c > 1$ and the lowest values are found in south part with $K_c < 1$.

The aggregation of crop coefficient K_c with respect to land-cover map results in the average values reported in Table 2. These averages are in good agreement with K_c values corresponding to the midseason stage recommended by (Allen et al. 1998). Their correlation coefficient is high, equal to 0.9 (Figure 7). Highest values of K_c are found for the forestland. The intermediate values correspond to the cropland and the lowest value is noted for the urban lands.

PET calculated with PM (PET_PM) is compared to the corrected pan observations (PET_PE). The estimation of these two methods for the first decade of March 2010 is

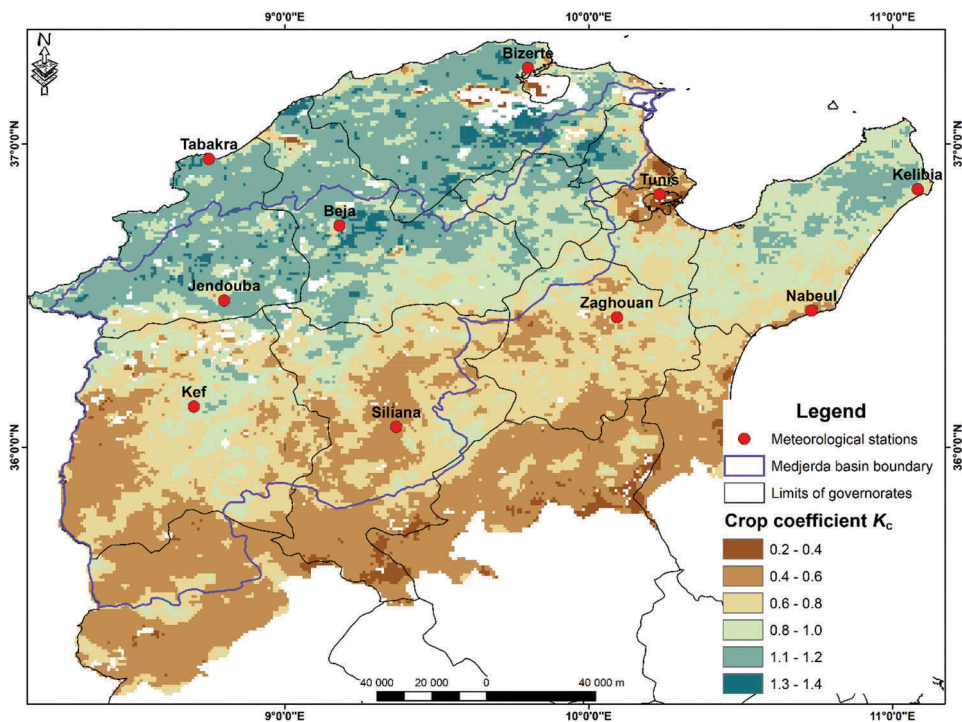
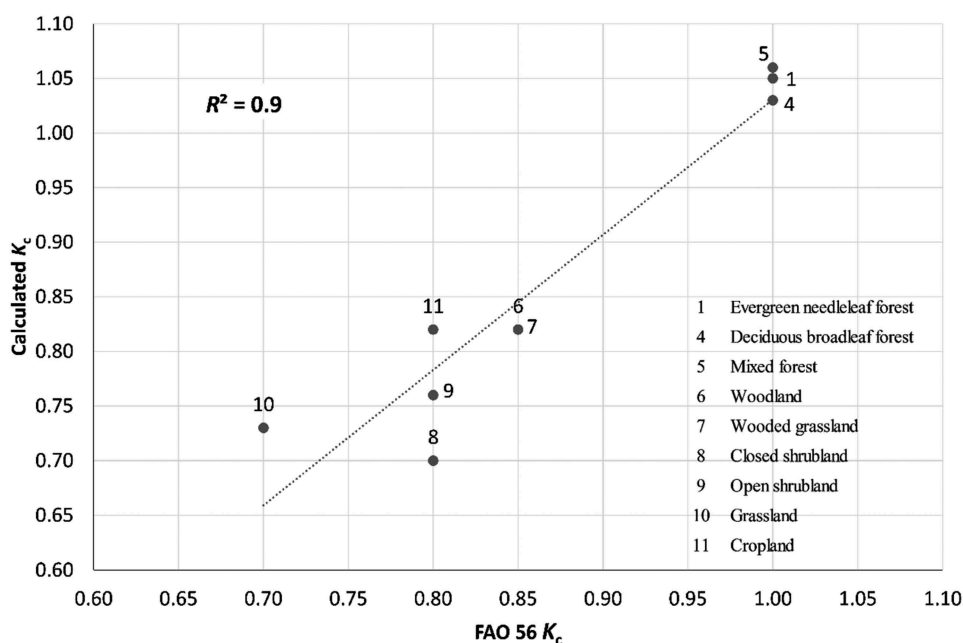


Figure 6. Map of crop coefficient K_c calculated on the base of NDVI and FVC maps for the first decade of March 2010.

Table 2. The average values of K_c for each land cover.

Code	Land-cover type	Calculated K_c	FAO 56 K_c
1	Evergreen needleleaf forest	1.05	1
4	Deciduous broadleaf forest	1.03	1
5	Mixed forest	1.06	1
6	Woodland	0.82	0.85
7	Wooded grassland	0.82	0.85
8	Closed shrubland	0.70	0.8
9	Open shrubland	0.76	0.8
10	Grassland	0.73	0.7
11	Cropland	0.82	0.8
14	Urban and built	0.53	-

**Figure 7.** Scatter plot of Crop coefficient (K_c) calculated for the first decade of March 2010 based on NDVI and FVC maps and aggregated according to the land use versus crop coefficient values (FAO 56 K_c) recommended by Allen et al. (1998) for the mid-season.

presented, respectively, in Figure 8(a) and Figure 8(b). The spatial distribution of PET for the first decade of March 2010 presents a variation between 0.6 and 3.3 mm in Figure 8(a) and between 1.2 and 3.3 mm in Figure 8(b) with an increase from south to north for both maps.

Further, a comparison is realized pixel per pixel. A good coefficient of determination is obtained $R^2 = 0.8$ for the first decade of March (Figure 9(a)). The same treatment is performed for the first decade of May and results of $R^2 = 0.7$, which is still quite satisfactory (Figure 9(b)).

Another comparison based on the land use is realized. It consists of aggregating the PET values of the first decade of March and May for each land use type. Twenty kinds of land cover are considered in Medjerda basin. The result of aggregation is reported in

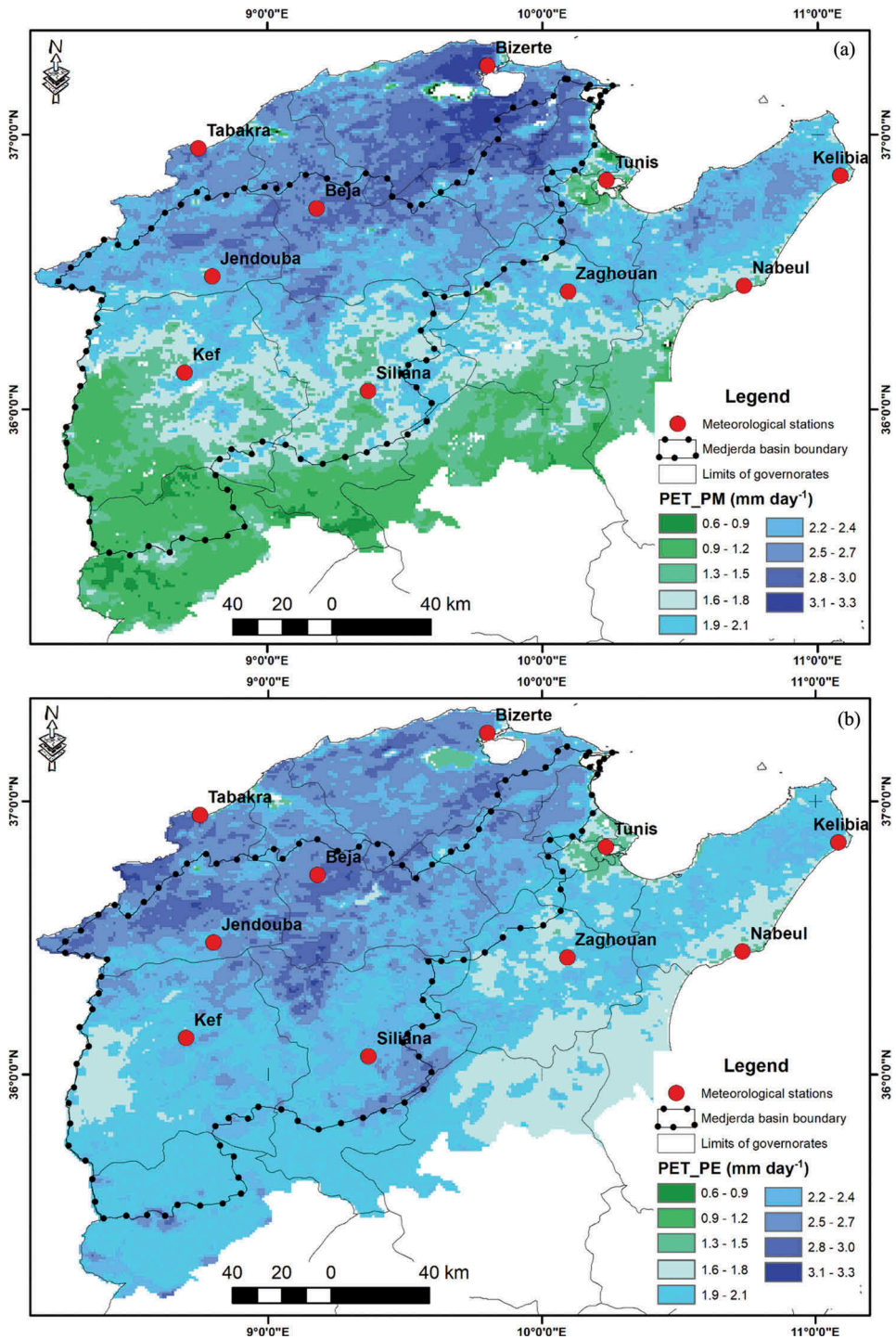


Figure 8. Map of decadal average potential evapotranspiration estimated, for the first decade of March 2010 based on (a) Penman–Monteith model, (b) pan evaporation (PE) and fraction of vegetation cover (FVC).

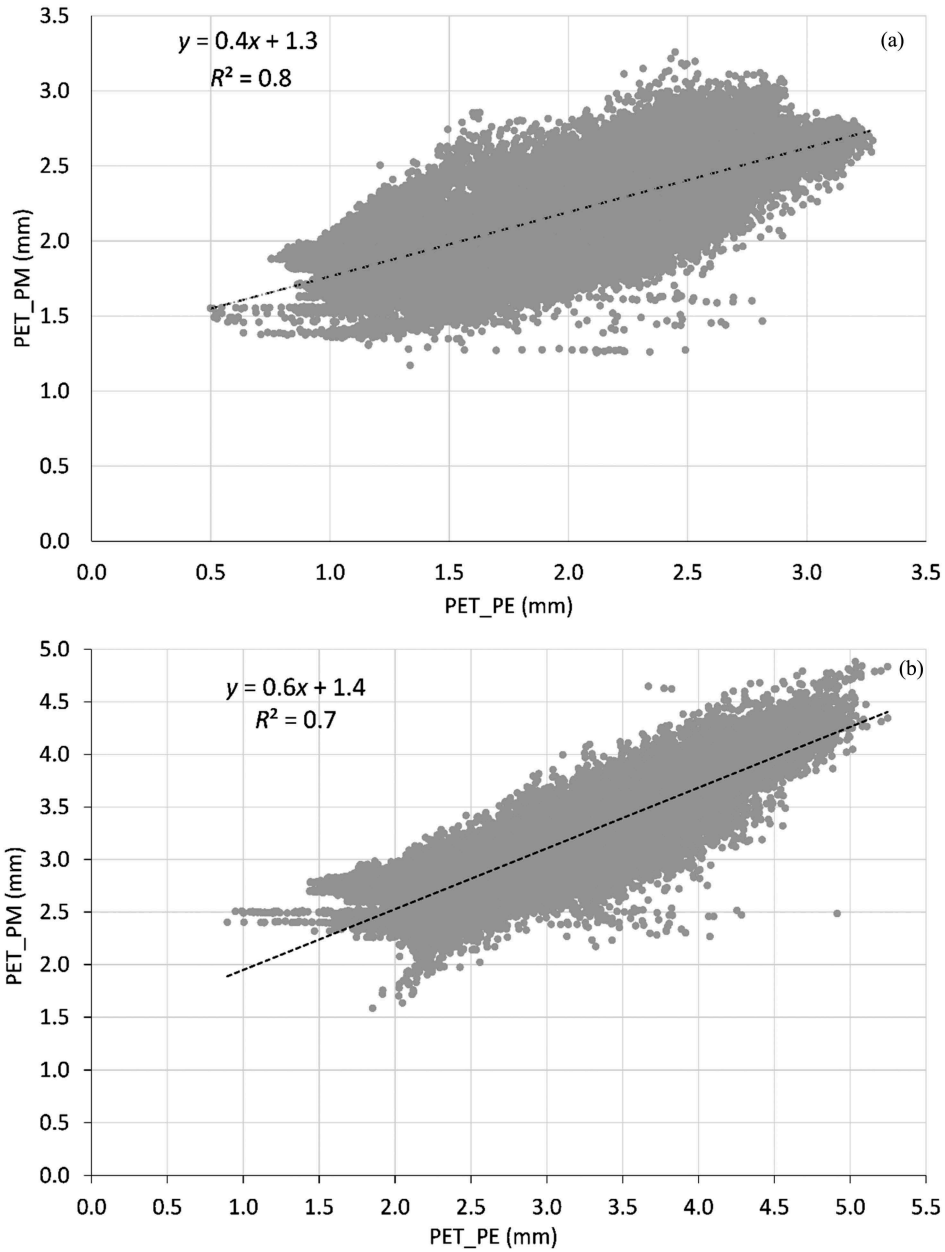


Figure 9. Scatter plot of PET_PM against PET_PE (a) for the first decade of March 2010 and (b) for the first decade of May 2010.

Figure 10. The coefficient of determination is about 0.7 for the first decade of March and 0.9 for the first decade of May, showing a good accuracy. However, for the first decade of March (Figure 10(a)), all the aggregated PET_PM are less than those estimated by corrected PE values. In addition, for the first decade of May, the aggregated values of PET_PM show a different trend (Figure 10(b)): only decadal PET_PM values of mosaic

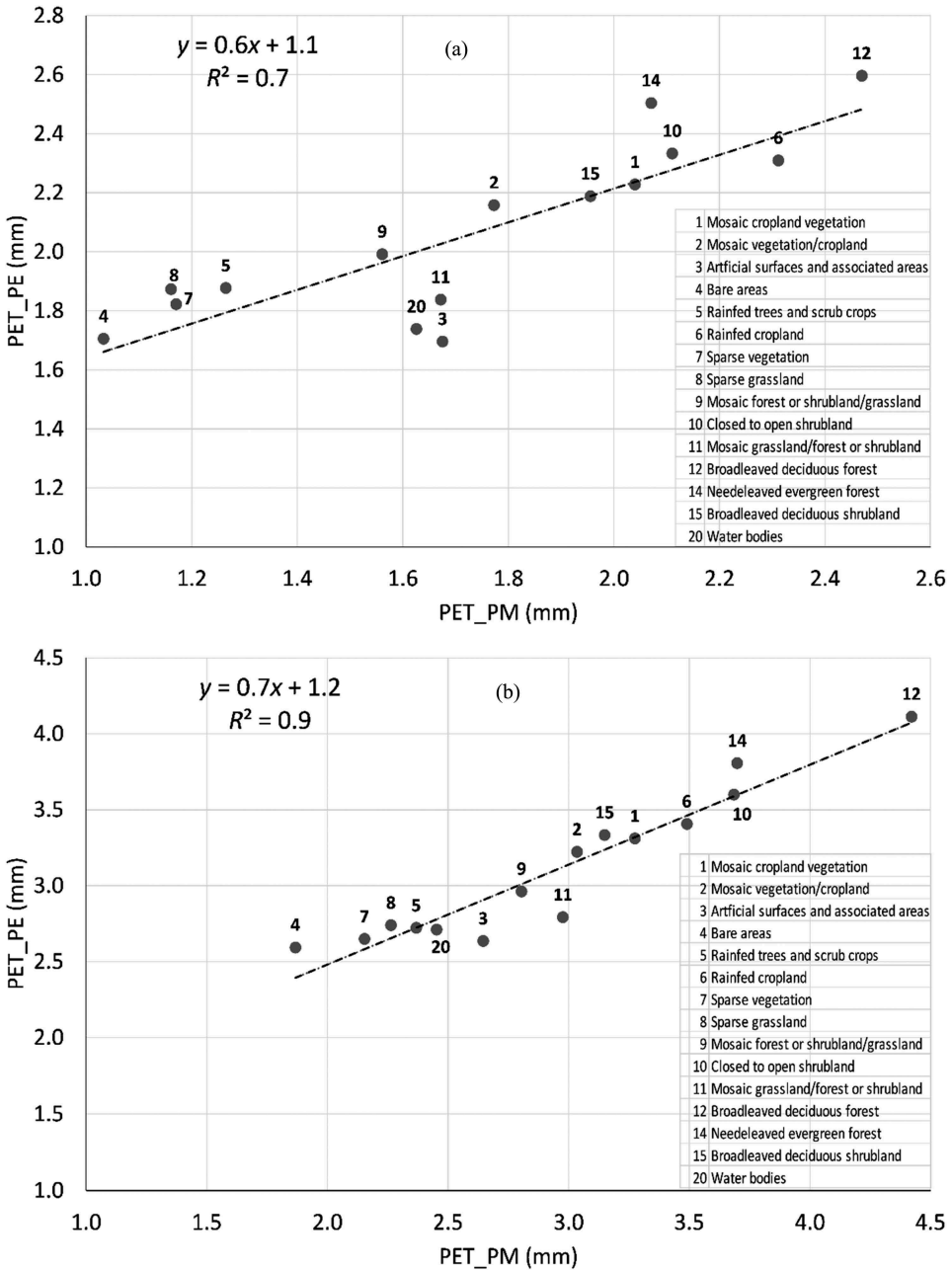


Figure 10. Scatter plot of decadal potential evapotranspiration for (a) March (1–10) and (b) May (1–10) aggregated for each land use in northern Tunisia.

grassland, rainfed cropland, closed to open shrubland, and closed broad-leaved deciduous forest are higher than PET_{PE} values. Despite this discrepancy and based on determination coefficients, it is assumed that the PET estimates by PM using satellite data is accepted and congruent the reality.

4.3. Temporal variability of evapotranspiration ET_0 , PET, and AET_LSA SAF

In order to validate the temporal variability of decadal sums of the PET estimations and of the AET-LSA SAF product, the results are recapitulated into graphs in comparison to decadal means of air temperature, relative humidity, and duration of sunshine. Some specific pixels are examined. For these pixels, the nearest meteorological station is adopted for comparison. From the sylvo-pastoral areas, mosaic forest or shrubland/grassland, broad-leaved deciduous forest, and sparse vegetation are studied. From cropland cover, rainfed cropland and Mosaic cropland vegetation are studied.

Figure 11(a) presents a comparison for a pixel from the broad-leaved deciduous forest. The reference and PET show the same trend with the PET superior to ET_0 in all decades, which can be explained by the crop coefficient K_c of forestland, which is up to one for all the year. In addition, the trend of variation of evapotranspiration shows an agreement with the temporal variation of air temperature, duration of sunshine, and relative humidity. Each increase peak is explained by an increase in air temperature and duration of sunshine with a decrease in relative humidity. For the mosaic forest or shrubland/grassland and the sparse vegetation (Figure 11(b) and Figure 11(c)), which also refers to sylvo-pastoral system in Medjerda basin, the temporal variation of reference, PET and AET show the same trend with ET_0 superior to PET for all the decades and PET superior to AET for all the decades. Each increase peak is clarified by an increase in air temperature and duration of sunshine with a decrease in relative humidity.

For the cropland (Figure 12), two pixels with mosaic vegetation and rainfed cropland are selected to observe the temporal variability of evapotranspiration and meteorological parameters. For this land-cover type, the potential and reference evapotranspiration represent different variations. For the first five decades of the year (initial stage), the PET varies under the ET_0 curve. From the sixth decade until the decade 12, the PET curve varies below the ET_0 curve. For the other decades, the PET decreases and ET_0 increase progressively. As the period, varying between the decade 5 and the decade 12 corresponds to the crop development stage and the mid-season stage, the crop coefficient K_c is up to 1. Therefore, the variation of evapotranspiration is explained by the variation of the crop coefficient.

4.4. Validation of water stress coefficient K_s

The evolution of the coefficient of determination R^2 is examined decade by decade (Figure 13). R^2 equal to 0.5 is obtained for the last decade of March and the first decade of April and then it decreases to 0.3. It increases again in the first decade of May. For the mid and the last decades of May, the coefficient of determination reaches its maximum value 0.8. So, the second and the third decades of May are best related to in-situ assessment ($R^2 > 0.7$). Awkwardly, the comparison is less satisfactory for the last decade of March and the first decade of April, which are helpful for early warning ($R^2 < 0.7$). However, the result ($R^2 = 0.5$) is not too bad.

Figure 14 highlights the variation of average K_s and F_a for each land-cover type for the first decade of April ($R^2 = 0.5$). For the cropland type, the values are close to the regression curve, which is very important as the in situ drought investigation concerns essentially the crop. Therefore, the first decade of April (mid stage) can give a

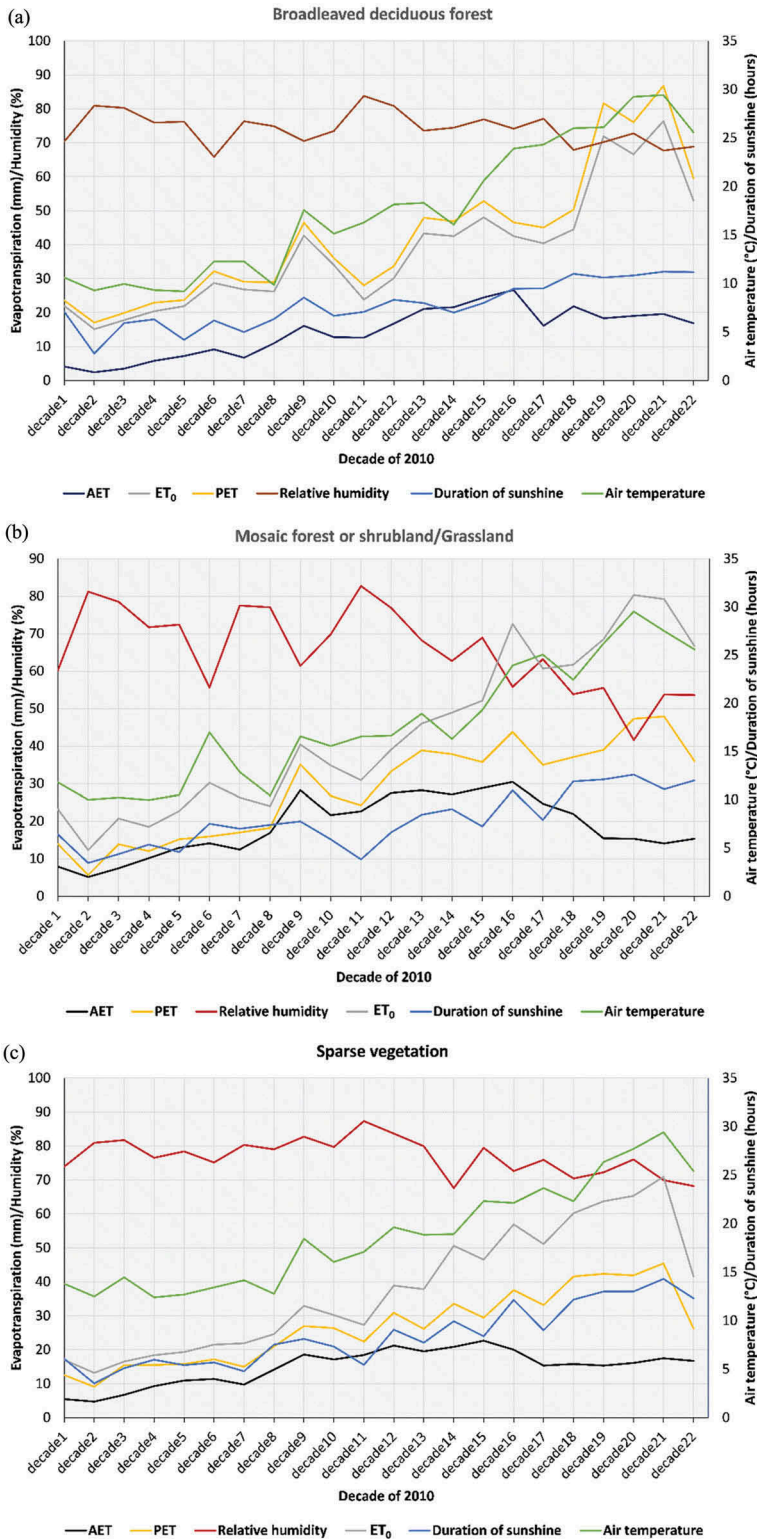


Figure 11. Temporal variability of evapotranspiration (AET/PET/ET₀), air temperature, relative humidity and duration of sunshine refer to sylvo-pastoral system: (a) broad-leaved deciduous forest, (b) mosaic forest or shrubland/grassland, (c) sparse vegetation in Medjerda Basin.

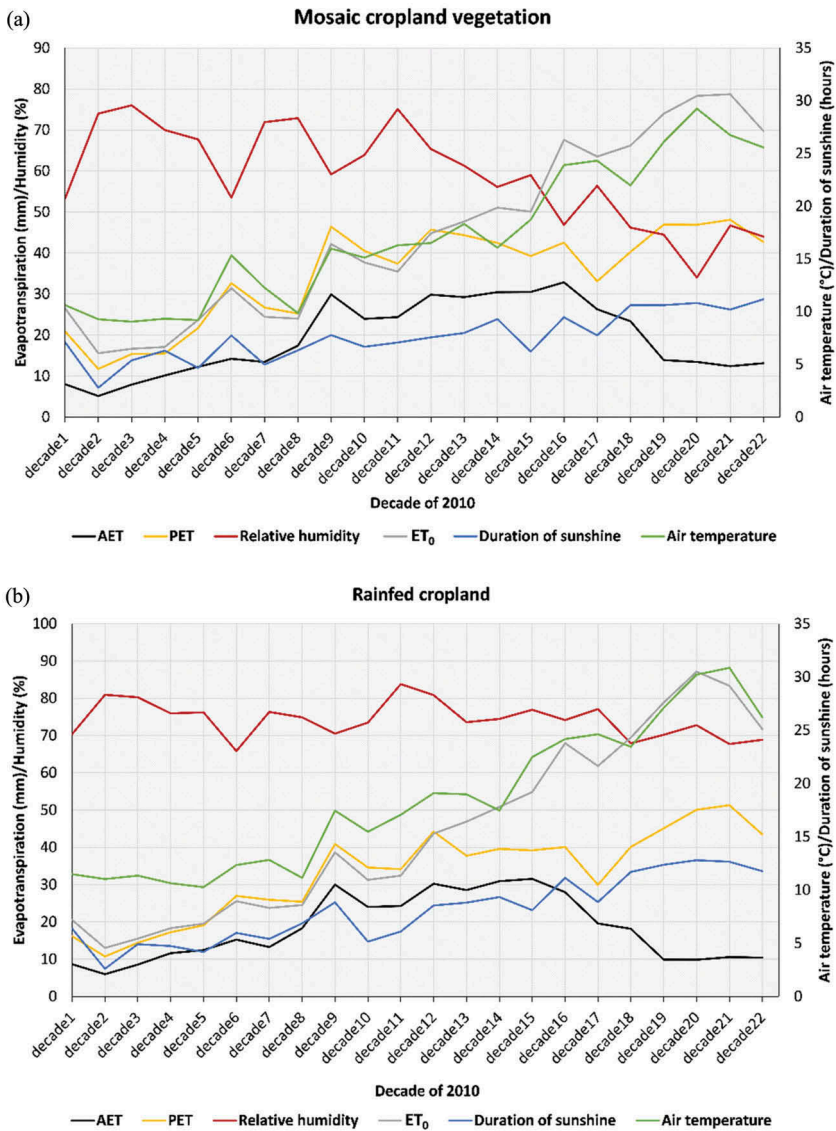


Figure 12. Temporal variability of evapotranspiration (AET/PET/ET₀), air temperature, relative humidity, and duration of sunshine in cropland cover: (a) mosaic cropland vegetation, (b) rainfed cropland in Medjerda Basin.

preliminary idea on the state of drought in the study area, particularly for the cropland. At the contrary, for the sylvo-pastoral systems, the values are scattered far from the curve especially for the forestland and the sparse grassland with no potential for drought early warning.

Figure 15 shows the variation of K_s and F_a for each land-cover type for the second and third decades of May ($R^2 = 0.8$). Satellite imagery estimations for sylvo-pastoral areas and croplands are situated on the regression curve. So, they can be considered as accurate indicators on the state of drought in these types of land cover in May (last stage).

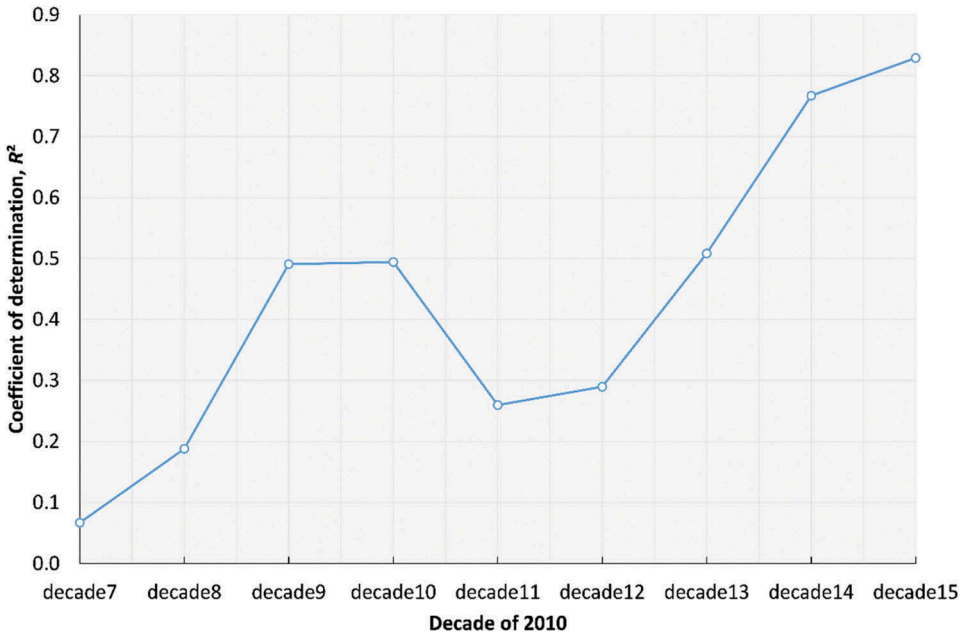


Figure 13. Coefficient of determination resulting from comparison of water stress coefficient calculated using remote sensing and the fraction of affected areas from decade 7 (first decade of March) to decade 15 (third decade of May).

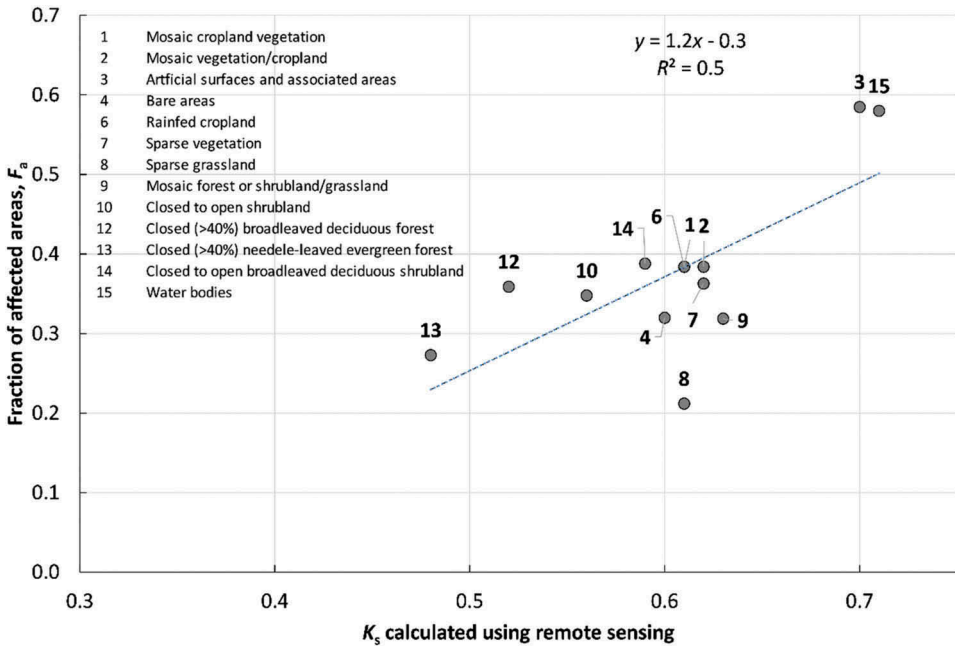


Figure 14. Scatter plot of fraction of affected areas and water stress coefficient calculated using remote sensing data aggregated by land cover in the Medjerda basin for the first decade of April (decade 10), 2010.

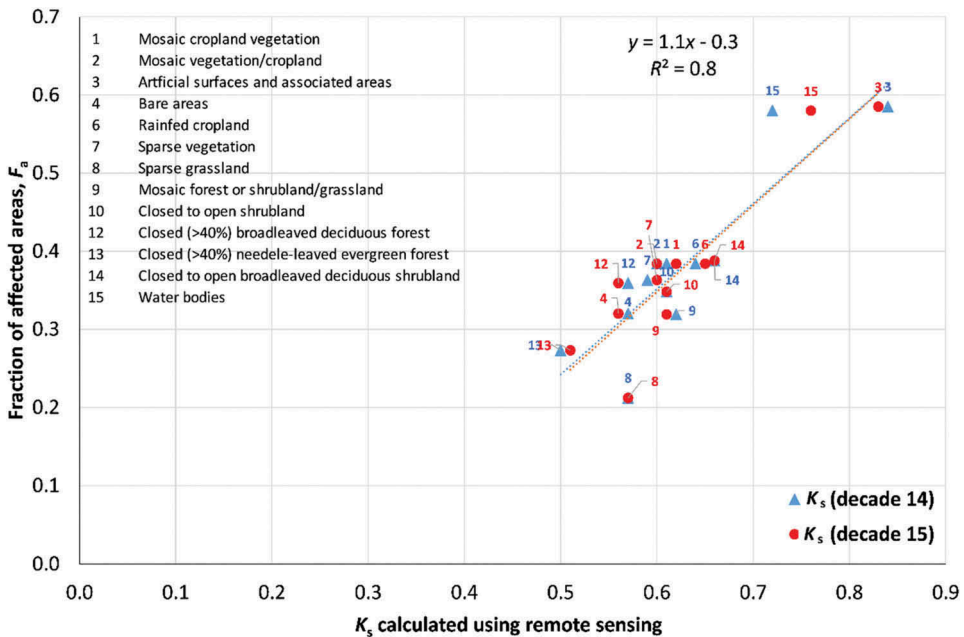


Figure 15. Scatter plot of fraction of affected areas and water stress coefficient calculated using remote sensing data aggregated by land cover in the Medjerda basin for the second and the third decade of May (decade 14 and 15), 2010.

5. Conclusion

Water stress coefficient K_s initiated by Allen et al. (1998) is determined for the study area. To achieve the computation of K_s , the FAO-56 PM model is used to estimate reference and PET. This approach is combined with optical remote-sensing data (NDVI SPOT-VGT, and FVC LSA SAF) for the assessment of the crop coefficient K_c , applying an empirical relationship. The resulting calculated PET is compared to corrected PE observations using the FVC-LSA SAF data. On the other hand, the AET is derived from LSA SAF product. Finally, the water stress coefficient is calculated for the year 2010 and aggregated by the land-cover type for the Medjerda basin and it is compared to the fraction of affected area published by the ministry of agriculture in the national official journal, which is linked to cropland yield deficit. Two main types of vegetation cover, cropland, and silvo-pastoral lands are considered in this analysis at the decadal scale.

The calculated crop coefficient (K_c) shows a good correlation ($R^2 = 0.9$) with values proposed by Allen et al. (1998) for the mid-season stage. The comparison between the corrected PE and calculated PET shows a good accuracy for the first decade of March and May 2010 with R^2 equal to 0.7 and 0.8, respectively. For the water stress coefficient, the comparison with in situ drought investigation indicates that the third decade of March and the first decade of April give a primary idea on the drought amplitude for the croplands. From May, remote-sensing data give accurate information for the identification of drought for both croplands and silvo-pastoral areas. Therefore, water stress coefficient calculated using optical remote-sensing data could be considered as a good indicator of drought for a different type of land cover in the Medjerda basin.

The study can help the authorities to detect the amplitude of drought as soon as possible in the different land-cover types and allows, as consequence, to predict the right decision to manage it.

Acknowledgments

The authors would like to thank University of Tunis El Manar for funding two months training of N. Abid in ITC and to thank ITC staff for their help during the training. They also thank the Ministry of agriculture, hydraulic resources, and fisheries; the National Institute of Meteorology (INM) in Tunis and General Direction of Dams and Large Hydraulic Works, Ministry of Agriculture.

This research was part PEER project (2015) "Contribution to drought identification and alert in Northern Tunisia" (http://sites.nationalacademies.org/PGA/PEER/PEERscience/PGA_084029).

Disclosure statement

No potential conflict of interest was reported by the authors.

Funding

The authors would like to thank Université de Tunis El Manar for funding two months training of N. Abid in ITC.

ORCID

Nesrine Abid  <http://orcid.org/0000-0001-6866-7096>

Zoubeida Bargaoui  <http://orcid.org/0000-0003-4737-2373>

Chris M. Mannaerts  <http://orcid.org/0000-0001-7882-8754>

References

- Allen, R. G., L. S. Pereira, D. Raes, and M. Smith (1998). Crop Evapotranspiration - Guidelines for Computing Crop Water Requirements - FAO. Irrigation and Drainage Paper 56, FAO Rome. Retrieved from <http://www.fao.org/docrep/X0490E/X0490E00.htm>.
- Allen, R. G., W. Pruitt, D. Raes, M. Smith, and L. Pereira. 2005. "Estimating Evaporation from Bare Soil and the Crop Coefficient for the Initial Period Using Common Soils Information." *Journal Irrig Drain Engineering* 131 (1): 14–23. doi:10.1061/(ASCE)0733-9437(2005)131:1(14).
- Amri, R., M. Zribi, B. Duchemin, Z. Lili-Chabaane, C. Gruhier, and A. Chebouni. 2011. "Analysis of Vegetation Behavior in a Semi-Arid Region Using SPOT-VEGETATION NDVI Data." *Remote Sens* 3 (12): 2568–2590. doi:10.3390/rs3122568.
- Amri, R., M. Zribi, Z. Lili-Chabaane, C. Szczypta, J. C. Calvet, and G. Boulet. 2014. "FAO-56 Dual Model Combined with Multi-Sensor Remote Sensing for Regional Evapotranspiration Estimations." *Remote Sens* 6: 5387–5406. doi:10.3390/rs6065387.
- Baccour, H., H. Feki, M. Slimani, and C. Cudennec. 2012. "Interpolation De L'évapotranspiration De Référence En Tunisie Par La Méthode De Krigeage Ordinaire." *Sècheresse* 23: 121–132. [In french]. doi:10.1684/sec.2012.0334.
- Boudabous, A., A. Jarraya, S. Nouira, and H. Bouzgaya (2000). Etude Nationale De La Diversité Biologique De La Tunisie. Monographie Tome II. Tunis: ministère de l'Environnement et de l'Aménagement du Territoire. 300p. [In French].

- Brown, J. F., B. D. Wardlow, T. Tadesse, M. J. Hayes, and B. C. Reed. 2008. "The Vegetation Drought Response Index (Vegdri): A New Integrated Approach for Monitoring Drought Stress in Vegetation." *GIScience and Remote Sensing* 45 (1): 16–46. doi:10.2747/1548-1603.45.1.16.
- Choi, M., J. M. Jacobs, M. C. Anderson, and D. D. Bosch. 2013. "Evaluation of Drought Indices via Remotely Sensed Data with Hydrological Variables." *Journal of Hydrology* Volume 476: Pages 265–273. doi:10.1016/j.jhydrol.2012.10.042.
- Dalezios, N. R., A. Blanta, and N. V. Spyropoulos. 2012. "Assessment of Remotely Sensed Drought Features in Vulnerable Agriculture." *Natural Hazards Earth Systems Sciences* 12: 3139–3150. doi:10.5194/nhess-12-3139-2012.
- Er-Raki, S., A. Chehbouni, G. Boulet, and D. G. Williams. 2010. "Using the Dual Approach of FAO-56 for Partitioning ET into Soil and Plant Components for Olive Orchards in a Semi-Arid Region." *Agricultural Water Managed* 97: 1769–1778. doi:10.1016/j.agwat.2010.06.009.
- Er-Raki, S., G. Chehbouni, N. Guemouria, B. Duchemin, J. Ezzahar, and R. Hadria. 2007. "Combining FAO-56 Model and Ground-Based Remote Sensing to Estimate Water Consumptions of Wheat Crops in a Semi-Arid Region." *Agricultural Water Managed* 87: 41–54. doi:10.106/j.agwat.2006.02.004.
- Ghulam, A., Z. L. Li, Q. Qin, Q. Tong, J. Wang, A. Kasimu, and L. Zhu. 2007. "A Method for Canopy Water Content Estimation for Highly Vegetated Surfaces—Shortwave Infrared Perpendicular Water Stress Index." *Sciences Chinese Series D: Earth Sciences* 50: 1359–1368. <https://link.springer.com/article/10.1007/s11430-007-0086-9>
- Habaieb, H., and C. H. Masmoudi-Charfi. 2003. Calcul Des Besoins En Eau Des Principales Cultures Exploitées Au Nord De La Tunisie: Estimation De L'Évapotranspiration De Référence Par Différentes Formules Empiriques (CAS Des Régions De Tunis, Béja Et Bizerte). [In French]. Retrieved from: http://www.iamm.ciheam.org/ress_doc/opac_css/index.php?lvl=notice_display&id=10147
- Hillel, D. 1997. *La Petite Irrigation Dans Les Zones Arides: Principes Et Options* (Document Publier Par Le FAO). Food & Agriculture 66. ISBN 92-5-203896-5. Retrieved from <http://www.fao.org/docrep/w3094f/w3094f00.htm>
- Hoerling, M., and A. Kumar. 2003. "The Perfect Ocean for Drought." *Science* 299 (5607): 691–694. doi:10.1126/science.1079053.
- Ji, L., and A. Peters. 2003. "Assessing Vegetation Response to Drought in the Northern Great Plains Using Vegetation and Drought Indices." *Remote Sens Environment* 87: 85–98. doi:10.1016/S0034-4257(03)00174-3.
- Kogan, F. N., Global drought watch from space. 1997. *Bulletin American Meteorol Social* 78: 621–636. Retrieved from <http://web.iitd.ac.in/~sagnik/C2.pdf>
- Masih, I., S. Maskey, F. E. F. Mussá, and P. Trambauer. 2014. "A Review of Droughts on the African Continent: A Geospatial and Long-Term Perspective." *Hydrol Earth Systems Sciences* 18: 3635–3649. doi:10.5194/hess-18-3635-2014.
- Neale, C. M. U., H. Jayanthi, and J. L. Wright. 2005. "Irrigation Water Management Using High-Resolution Airborne Remote Sensing." *Irrigation and Drainage System* 19: 321–336. Retrieved from <https://eurekamag.com/pdf.php?pdf=004445432>.
- Pereira, L. S., R. G. Allen, and A. Perrier. 2006. "Méthode Pratique De Calcul Des Besoins En Eau." In *Traité d'Irrigation*, Eds. J. R. Tiercelin and A. Vidal, 227–268. second ed. Paris: Éditions TEC & DOC, Lavoisier.
- Quiring, S. M., and S. Ganesh. 2010. "Evaluating the Utility of the Vegetation Condition Index (VCI) Formonitoring Meteorological Drought in Texas." *Agricultural Forest Meteorol* 150: 330–339. doi:10.1016/j.agrformet.2009.11.015.
- Riou, C., and R. Chartier. 1985. "Évapotranspiration En Zone Semi-Aride De Deux Couverts Végétaux (Gazon, Blé) Obtenue Par Plusieurs Méthodes. I. - Evaluation De L'ETP (Conditions Hydriques Non limitantes)." *Agronomie* 5 (3): 261–266. doi:10.1051/agro:19850308.
- Rocha, J., A. Perdigão, R. Melo, and C. Henriques. 2010. Managing Water in Agriculture through Remote Sensing Applications. Available at: https://www.researchgate.net/profile/Jorge_Rocha7/publication/228413258_Managing_Water_in_Agriculture_through_Remote_Sensing_Applications/links/00b7d533e978b95954000000.pdf.

- SAF. 2011. The EUMETSAT Satellite Application Facility on Land Surface Analysis (LSA SAF) Product User Manual Evapotranspiration (ET). Available at: <https://www.google.com/urlsa=t&rct=j&q=&esrc=s&source=web&cd=4&cad=rja&uact=8&ved=0ahUKEwjgKJPFoO7YAhVPyqQKHaBOC3sQFgg6MAM&url=https%3A%2F%2Flandsaf.ipma.pt%2FGetDocument.do%3Ffid%3D613&usg=AOvVaw2LhITApPio0f-tJVoRj3r>
- Seiler, R. A., F. Kogan, and G. Wei. 2000. "Monitoring Weather Impact and Crop Yield from NOAA AVHRR Data in Argentina." *Advancement Space Researcher* 26: 1177–1185. doi:10.1016/S0273-1177(99)01144-8.
- Tadesse, T., J. F. Brown, and M. J. Hayes. 2005. "A New Approach for Predicting Drought-Related Vegetation Stress: Integrating Satellite, Climate, and Biophysical Data over the U.S. Central Plains." *ISPRS Journal of Photogrammetry and Remote Sensing* 59 (4): 244–253. doi:10.1016/j.isprsjprs.2005.02.003.
- Van Den Hurk, B. J. J. M., P. Viterbo, A. C. M. Beljaars, and A. K. Betts. 2000. "Offline Validation of the ERA40 Surface Scheme." *ECMWF TechMemo* 295: 42 pp. ECMWF, Reading <http://www.ecmwf.int/en/elibrary/12900-offline-validation-era40-surface-scheme>.
- Viterbo, P., and A. Beljaars. 1995. "An Improved Surface Parameterization Scheme in the ECMWF Model and Its Validation." *Journal Climate* 8: 2716–2748. doi:10.1175/1520-0442(1995)008<2716:AILSPS>2.0.CO;2.
- Wright, J. L. 1982. "New Evapotranspiration Crop Coefficients." *Journal of Irrigation and Drainage* 108 (1): 57–7. https://www.researchgate.net/publication/279898461_New_Evapotranspiration_Crop_Coefficient.
- Zahar, Y. 1997. *Éléments D'hydrologie Pour L'aménagement. Modélisation spatiale et temporelle des précipitations extrêmes et érosives en Tunisie centrale*. Université de La Manouba - Volume V, 287 pages. Imprimerie officielle de la république tunisienne. I.S.B.N. 9973-936-13-2. [In French].
- Zargar, A., R. Sadiq, and B. Naser. 2011. "A Review of Drought Indices." *Environmental Review* 19: 333–349. [In French]. doi:10.1139/A11-013.